Evidence for Island Structures as the Dominant Architecture of Asphaltenes

Hassan Sabbah,[†] Amy L. Morrow,[†] Andrew E. Pomerantz,[‡] and Richard N. Zare*,[†]

[†]Department of Chemistry, Stanford University, Stanford, California 94305, United States
[‡]Schlumberger-Doll Research, Cambridge, Massachusetts 02139, United States

ABSTRACT: Laser desorption laser ionization mass spectra of 23 model compounds and 2 petroleum asphaltene samples are presented. These experiments involved desorption by irradiation with the 10.6 μm output of a CO_2 laser followed by single-photon ionization with the 157 nm output of a fluorine excimer laser. The average molecular weight of the asphaltene samples agrees closely with that found previously using multiphoton ionization with the 266 nm output of a Nd:YAG laser. The fragmentation behavior as a function of ionization laser pulse energy is studied to evaluate which families of model compounds fragment differently from asphaltenes and, hence, can be excluded from being dominant in asphaltenes. All model compounds having one aromatic core with and without various pendant alkyl groups show little to no fragmentation, mimicking the behavior observed for the two asphaltene samples, whereas all model compounds having more than one aromatic core show energy-dependent fragmentation. These observations support the contention that the dominant structural character of asphaltenes is island-like.

■ INTRODUCTION

Asphaltenes compose a fraction of petroleum defined by their insolubility in *n*-pentane or *n*-heptane and solubility in benzene or toluene. This fraction is a very complex mixture of polycyclic aromatic hydrocarbons (PAHs) variably substituted with alkyl groups and heteroatoms, including nitrogen, sulfur, oxygen, nickel, and vanadium. Asphaltene elemental composition is well-defined. Furthermore, most mass spectrometric techniques as well as molecular diffusion techniques now produce an asphaltene molecular-mass distribution peaking near 600−750 Da.[1−9] Despite these recent advances in understanding asphaltene characteristics, the molecular structures dominating asphaltenes remain poorly understood.

Two competing models have been proposed to describe the dominant molecular architectures in asphaltenes. First is the "archipelago" model,[10,11] in which several aromatic moieties are bridged together via aliphatic chains. Second is the "island" or Yen−Mullins model,[6,9,12] in which asphaltene molecules contain one polyaromatic core with pendant aliphatic chains. The on-going debate centers on the question of dominance: do the majority of individual asphaltene molecules conform to one or the other of these two models?

To address this issue, we continued our investigations[13] into different families of compounds, including linked-pyrene model compounds, single-pyrene model compounds, linked-phenanthrene model compounds, cholestanone model compounds, porphyrins, and PAHs (see Tables 1 and 2). These compounds were selected because they are the best representatives of island and archipelago compounds that we could find. It is not always clear-cut whether a compound should be described as having an island or archipelago structure. We define model compounds with at least 2 similarly sized aromatic cores connected by an aliphatic chain as archipelagos; otherwise, they are considered as islands. Hence, the cholestanone model compounds, containing benzenes linked to a larger aromatic core, are considered as

islands. Mass spectrometric analysis took place at Stanford University, where the fragmentation behavior of each model compound was compared to that of asphaltenes through application of two-step laser desorption laser ionization mass spectrometry (L²MS). The aim of this study is to eliminate, to the extent possible, candidate structures from being proposed as the dominating asphaltene molecular architecture.

With the L²MS technique, an infrared laser (λ = 10.6 μm) pulse is employed to generate a plume of gas from the surface of a solid sample. The generated plume is free of ions because the photon energy ($\sim$0.1 eV) of the employed laser is 2 orders of magnitude below the ionization threshold of any molecule potentially present in asphaltenes and the intensity of the laser pulse is maintained below the threshold for plasma formation. The absence of strong ion-induced dipole attractive forces in the plume suppresses aggregation.[14] After an appropriate time delay, the output from a fluorine excimer laser (λ = 157 nm) intersects the plume of neutral species and ionizes species with ionization potentials less than 7.89 eV, the energy of a single photon. The photon energy of the excimer laser is sufficient to ionize most potential constituents of asphaltenes. We believe that single-photon ionization (SPI) at 157 nm is a major improvement over resonance-enhanced multiphoton ionization (REMPI) at 266 nm because SPI puts less internal energy (1.43 eV) into the ionized molecule and therefore minimizes fragmentation.

In this work, we apply the SPI L²MS technique to six families of model compounds as well as to two petroleum asphaltene samples. The results that we obtain suggest an upper limit of 1500 Da for the molecular mass of asphaltene molecules. Most importantly, we compare the fragmentation behavior of the model compounds to that of asphaltenes. This comparison

Table 1. Nomenclature and Structures of the Model Compounds That Have Archipelago (A) Architecture

Name	Structure	MW(g/mol)
1,4-dipyren-1-yl-butane (A-1)		460
1,4-Bis(2-pyren-1-yl-ethyl)-benzene (A-2)		534
2,6-Bis(2-pyren-1-yl-ethyl)-pyridine (A-3)		535
2,5-Bis(2-pyren-1-yl-ethyl)-thiophene (A-4)		540
4,4'-Bis(2-pyren-1-yl-ethyl) -2,2'-bipyridine (A-5)		612
5,5'-Bis(2-pyren-1-yl-ethyl) -2,2'-bithiophene (A-6)		622
2,7-Bis(2-pyren-1-yl-ethyl)- 9,9-diethyl-9H-fluorene (A-7)		678
3,5-Bis(2-phenanthr-9-yl-ethyl)-pyridine (A-8)		487
2,6-Bis(2-phenanthr-9-yl-ethyl)-pyridine (A-9)		487
5,5'-Bis(2-phenanthr-9-yl-ethyl) -2,2'-bithiophene (A-10)		574

suggests that the island molecular architecture dominates asphaltenes.

■ EXPERIMENTAL SECTION

Model Compounds. The linked-pyrene model compounds, single-pyrene model compounds, linked-phenanthrene model compounds, and cholestanone model compounds were synthesized as described previously.[13] All other compounds were purchased from Sigma-Aldrich (St. Louis, MO). All compounds were used as received.

Asphaltene Samples. Asphaltenes were extracted from two Middle Eastern black oils following standard procedures. Briefly, the oil was diluted 1:40 in *n*-heptane, and the solution was stirred overnight. Asphaltene particles were then extracted from solution by vacuum filtration over a nylon filter with 1.2 μm pores. The resulting asphaltenes were then washed in a Soxhlet extractor using *n*-heptane for 1 week to remove any *n*-heptane-soluble co-precipitates.

L^{2}MS. L^{2}MS has been described in detail elsewhere.[15,16] In this section, we provide a brief description of the apparatus and the recently upgraded ionization method.
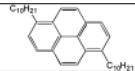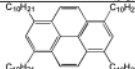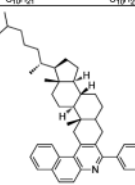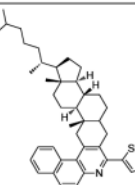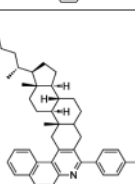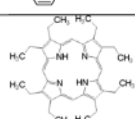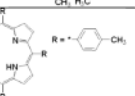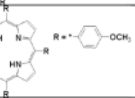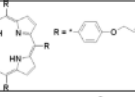
For L^{2}MS analysis, the samples are prepared as described in our previous work.[13] Once the sample solution has completely dried, the sample is introduced inside the mass spectrometer via a vacuum interlock and mounted on an XYZ manipulator. This manipulator allows us to align the sample within the ion extraction region of the mass spectrometer and grants us the ability to probe different locations on the sample surface. Once inside the mass spectrometer chamber, the sample is observed by a charge coupled device (CCD) camera via a germanium dichroic mirror. Molecules from the solid surface of the sample are desorbed by a pulse of infrared (IR) light ($\lambda = 10.6\,\mu$m) from a CO$_2$ laser (Alltech AL 882 APS). The laser pulse is characterized by a 120 ns full
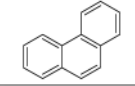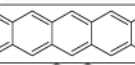
width at half-maximum Gaussian peak with 4 μs tail. A Cassegrainian microscope objective (Ealing Optics, 15×) is employed to focus the IR laser beam to a spot of 50 μm. The heating rate induced by the pulsed IR laser focused on the sample surface is approximately 10^8 K/s.[17,18] This heating rate is far more rapid than that of resistive heating (10 K/s) and, thus, favors intact desorption over thermal decomposition.[17] The typical pulse energy range used for these experiments was 3−10 mJ/pulse.

A plume of desorbed neutral molecules requires 10−50 μs to traverse the distance, approximately 2 mm, separating the sample from the extraction region. Once this plume expands into the extraction region, an ultraviolet (UV) laser beam at 266 nm or a vacuum ultraviolet (VUV) laser beam at 157 nm intersects the plume to ionize the neutral molecules. The former ionization source is the fourth harmonic ($\lambda = 266$ nm; $E_{photon} = 4.66$ eV) of a Nd:YAG laser (Spectra Physics DCR11; 10 ns pulse width; 10 Hz repetition rate), which causes [1 + 1] REMPI. This technique is considered as a soft ionization technique for aromatic hydrocarbons because the total energy deposited is only 9.32 eV.

The new ionization source, which has been recently coupled to the apparatus, is a fluorine excimer laser (ExciStar XS 200) that generates VUV light at 157 nm ($E_{photon} = 7.89$ eV) for single-photon ionization. SPI does not require resonant absorption to an intermediate electronically excited state and is a universal ionization technique for any molecule with an ionization potential (IP) below the photon energy.[20] Once the ionization potential threshold is exceeded, the ionization cross-section of PAHs is proportional to the number of carbon atoms,[19] eliminating the ionization dependence upon unknown absorption cross-sections of excited molecular states. Thus, a more quantitative analysis is accessible with this technique. Furthermore, the photon energy of the fluorine excimer laser is less than that of the two-photon REMPI process by 1.43 eV. This difference of energy deposited in the molecule makes SPI a softer ionization technique for many classes of organic compounds,

Table 2. Nomenclature and Structures of the Model Compounds That Have Island (I) Architecture

Compound	Structure	Mass
1,6-didecyl pyrene (I-1)		482
1,3,6,8-tetradecyl pyrene (I-2)		762
MCR-Cholestanone-Phenyl (I-3)		597
MCR-Cholestanone-Thiophen (I-4)		603
MCR-Cholestanone-Phenyl-n-Butyl (I-5)		653
2,3,7,8,12,13,17,18-Octaethyl-21H,23H-porphine (I-6)		534
5,10,15,20-Tetra-p-tolyl-21H,23H-porphine (I-7)		670
5,10,15,20-Tetrakis(4-methoxyphenyl)-21H,23H-porphine (I-8)		734
5,10,15,20-Tetrakis[4-(allyloxy)phenyl]-21H,23H-porphine (I-9)		839
Phenanthrene (I-10)		178
Pyrene (I-11)		202
Pentacene (I-12)		278
Coronene (I-13)		300

although the single-photon energy is sufficient to ionize nearly any potential component of asphaltenes.[20]

Once these ions are created, they are mass-analyzed using a home-built time-of-flight (TOF) mass spectrometer employing a modified Wiley–McLaren geometry.[21] The ion detector consists of a set of dual microchannel plates in a chevron configuration (MCPs; 20 cm^2 active area; Burle Electro-Optics, Sturbridge, MA) combined with a large collector anode (Gallileo TOF-400). A fast preamplifier (Ortec 93526) and a timing filter (Ortec 474) are used to amplify the generated ion signal. The amplified signal is averaged within the oscilloscope (Lecroy

9450) for a series of 50 sets of desorption and ionization laser shots for each recorded spectrum.

With the instrumental upgrade to SPI, calibration is required before analysis of complex, unknown samples can be reported with any confidence. To this end, we have completed a series of experiments, described below, which show the ability of SPI L^{2}MS to record mass spectra dominated by singly charged parent ion peaks and free from aggregation. Another serious issue regarding laser mass spectrometric techniques is that of comparing the behavior of analytes when probed separately or in a mixture. To come to a conclusion regarding the
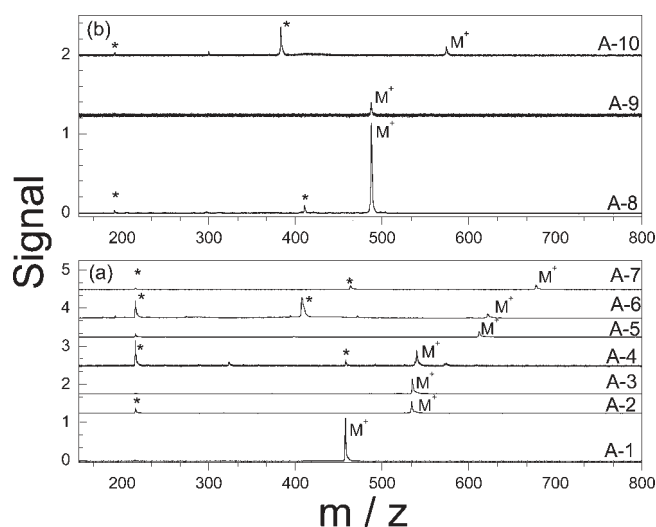
Figure 1. L^{2}MS mass spectra of two families of model compounds that have archipelago (A) architecture. The asterisks denote fragments of the indicated parent ions (M$^+$). All mass spectra presented here were recorded employing identical experimental parameters. (a) Linked-pyrene model compounds and (b) linked-phenanthrene model compounds. Compound identification is given in Table 1.

variation in desorption and ionization efficiencies for these model compounds in L^{2}MS, a mixture of synthetic model compounds as well as a mixture of asphaltenes with a model compound were prepared and analyzed. These experiments are discussed below and suggest that L^{2}MS is generally sensitive to most compounds believed to be asphaltene components.

Ability of SPI L^{2}MS To Detect Model Compounds without Fragmentation, Aggregation, or Multiple Charging. Figures 1 and 2 present SPI L^{2}MS mass spectra of all 23 compounds included in this study recorded using identical experimental conditions (3 mJ/pulse for desorption; 0.1 mJ/pulse for ionization). The singly charged parent ions (M$^+$) are observable in all of the SPI L^{2}MS mass spectra and dominant in most of them, including those in Figure 1a, where the parent ion was undetectable with REMPI L^{2}MS.[13] No aggregates have been detected, although if ionized aggregates had been present, we have demonstrated that this instrument does have the capability of detecting them over the mass range in which aggregates occur. These observations demonstrate that SPI L^{2}MS provides efficient and soft ionization for all compounds studied without the formation of aggregates or multiply charged species. This conclusion is the same as was obtained for the previous REMPI L^{2}MS study.[13]

Table 3 lists the abundance of the parent ion peak in each mass spectrum. This abundance is the ratio of the peak area (pa) calculated for the parent ion peak over the sum of the peak areas calculated for the parent ion peak and its related fragment(s). Table 3 shows that the abundance of the parent ion peak for all of the model compounds is comparable.

Ability of SPI L^{2}MS To Detect Most Components of Asphaltenes. Two mixtures were prepared to test the ability of L^{2}MS to detect simultaneously different types of compounds present in a single sample. The first mixture was an equimolar mixture of five model compounds, including I-2, I-5, I-6, I-8, and I-11. This mixture spans a mass range from 202 to 762 Da. Figure 3 presents the L^{2}MS spectrum of this mixture. Each peak is labeled by the model compound name and its normalized peak area (pa). The normalized pa of the different peaks is proportional to the sensitivity of SPI L^{2}MS to these compounds. All studied compounds are detected with nearly uniform sensitivity (within a factor of 3), in contrast to other ionization techniques, such as electrospray ionization, where the sensitivity varies

by orders of magnitude. The average molecular weight of this mixture is found to be 562 Da by the L^{2}MS technique, which agrees within 3% with the calculated average molecular weight of the equimolar mixture of 577 Da. This result shows that the combined variations in both desorption efficiency and ionization efficiency for these five compounds are relatively small and that L^{2}MS is capable of accurately measuring the molecular-mass distribution of a mixture.

Figure 4 presents the L^{2}MS spectrum of a mixture of asphaltenes and I-8, a porphyrin with mass 734 Da, in a 2:1 molar ratio. This ratio was determined by approximating the molecular mass of asphaltenes as the mass at which the L^{2}MS molecular-mass distribution peaks, 750 Da. The broad peak around 750 Da of the molecular-mass distribution of asphaltenes was not affected by the presence of a model compound with a similar mass. Integrating the asphaltene signal and the porphyrin signal yields the result that L^{2}MS is more sensitive to asphaltenes than to I-8 by a factor of 2.5. By comparison to the results of Figure 3, L^{2}MS detects asphaltenes more sensitively than I-2, I-5, I-8, and I-11, whereas L^{2}MS detects asphaltenes less sensitively than I-6. This result demonstrates that the detection efficiency for different molecules in L^{2}MS is constant within an order of magnitude and suggests that L^{2}MS is approximately equally sensitive to most components of asphaltenes. Taken together, Figures 3 and 4 indicate that SPI L^{2}MS is able to measure accurately the mass spectrum of components in a complex mixture and to estimate the molecular-mass distribution of a complex mixture, such as asphaltenes

■ RESULTS

Following these calibration studies, we present the SPI L^{2}MS asphaltene molecular-mass distribution. Then, we compare the fragmentation behaviors of both the model compound families and asphaltene samples.

Molecular-Mass Distribution of Asphaltene Molecules. The asphaltene molecular-mass distribution probed with SPI L^{2}MS is presented in Figure 5. This distribution extends to 1500 Da and is characterized by a broad peak around 750 Da (in approximate agreement[7,13,14] with a previous measurement using [1 + 1] REMPI at 266 nm). As with REMPI L^{2}MS,[7,13,14] the molecular-mass distribution of asphaltenes is found to be insensitive to changes in the pulse energy of the ionization laser, as shown by the different traces in Figure 5.

Fragmentation Behavior of Asphaltenes and Model Compounds. Mass spectra have been recorded over a range of ionization laser pulse energies (0.1−2 mJ/pulse) for each model compound listed in Tables 1 and 2 and for the two asphaltene samples BG5 and UG8. For each of these mass spectra, the peak area (pa) is calculated for the parent ion peak and also the related fragment peak(s). Then, for each specific ionization laser pulse energy, an average molecular weight (AMW) is calculated from

$$\text{AMW} = \frac{\sum\limits_i (\text{pa})_i \left(\dfrac{m}{z}\right)_i}{\sum\limits_i (\text{pa})_i} \tag{1}$$

where we sum over all mass peaks, i. Figure 6 plots the deduced AMW for each model compound and for each asphaltene sample versus the ionization laser pulse energy. Each data point of BG5 and UG8 asphaltenes presented in Figure 6 is the average of five repeated experiments. Error bars represent one standard deviation. The deduced AMW of asphaltenes exhibits little dependence upon ionization laser pulse energy (<1% in the range studied here). We conclude that asphaltenes do not fragment appreciably over the pulse energy range studied.
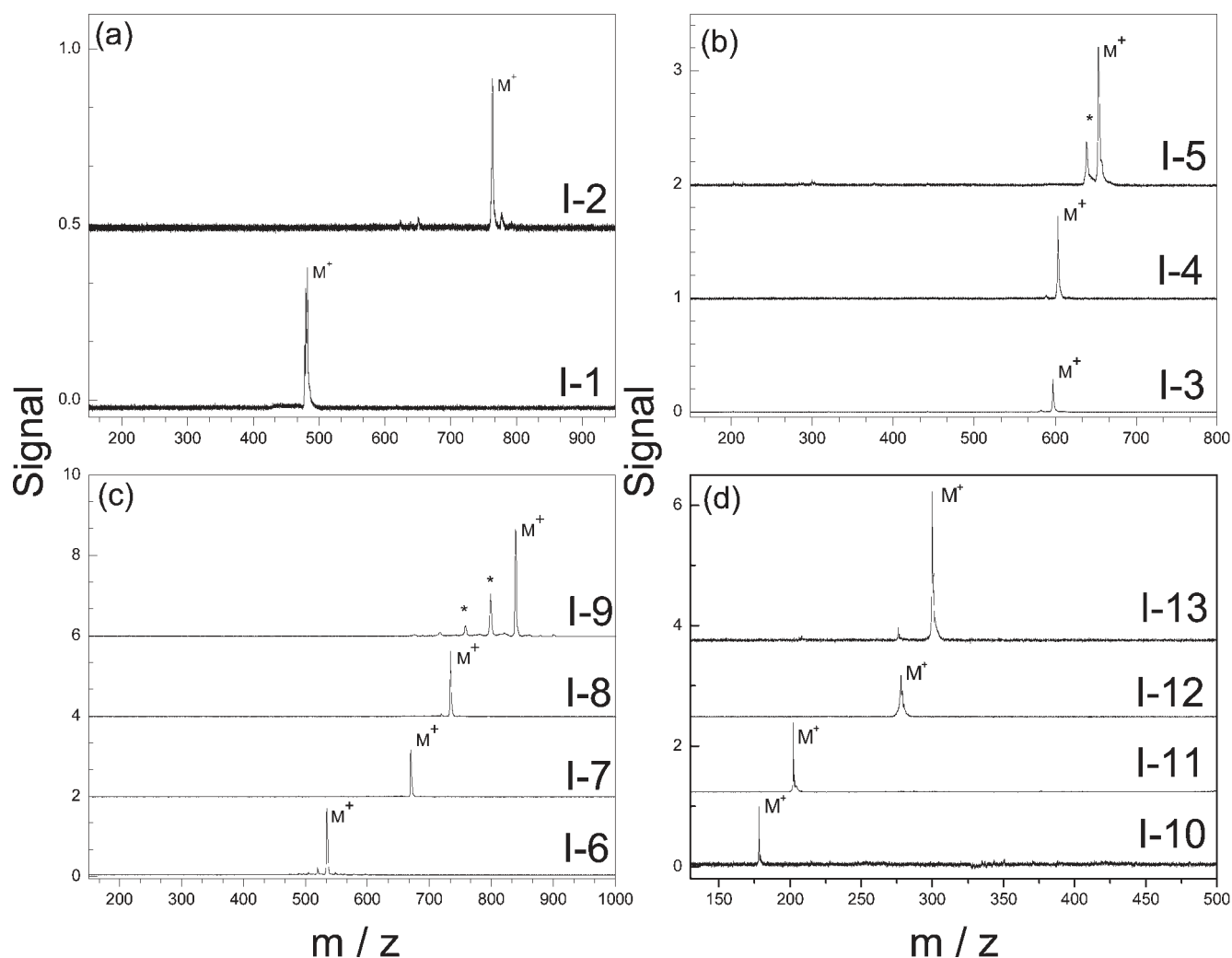
Figure 2. L^{2}MS mass spectra of four families of model compounds that have island (I) architecture. The asterisks denote fragments of the indicated parent ions (M$^+$). All mass spectra presented here were recorded employing identical experimental parameters. (a) Single-pyrene model compounds, (b) cholestanone model compounds, (c) porphyrins, and (d) PAHs. Compound identification is given in Table 2.

Two of the studied families in Figure 6 have multiple aromatic cores (2 or 3 aromatic cores per compounds) and represent archipelago molecules: linked-pyrene model compounds (A-1–A-6) and linked-phenanthrene model compounds (A-7–A-9). Both of these model compound families show fragmentation in L^{2}MS at high laser pulse energy, which results in a decrease in AMW with increasing pulse energy. The other four families of model compounds presented in Figure 6 have a single aromatic core and represent island molecules: model compounds with single-pyrene cores (I-1 and I-2), cholestanone derivatives (I-3–I-5), porphyrins (I-6–I-9), and PAHs (I-10–I-13). These four families of model compounds do not fragment in L^{2}MS and result in an AMW that does not change with laser pulse energy. The AMW of asphaltenes is also found to be unchanged with laser pulse energy; therefore, the fragmentation behavior of asphaltenes is similar to the single aromatic core compounds and different from the 2–3 aromatic core compounds.

The stability of the model compounds in L^{2}MS as a function of ionization laser pulse energy seems to be influenced strongly by the number of aromatic cores. However, other structural parameters of these model compounds, such as aromatic carbon percentage and H/C ratio, may also contribute to their fragmentation behavior. To

investigate the relative importance of these parameters in determining the fragmentation behavior of model compounds and asphaltenes, we prepared plots of the stability index (AMW at the lowest ionization laser pulse energy/AMW at the highest ionization laser pulse energy) of these compounds versus aromatic carbon percentage (Figure 7) and versus H/C ratio (Figure 8).

Figure 7 shows that model compounds with a single aromatic core resist fragmentation, regardless of the aromatic carbon percentage (stability index > 0.98 or so). Conversely, all model compounds studied with 2 or 3 aromatic cores fragment appreciably (stability index in the range of 0.5–0.9). Asphaltenes resist fragmentation (stability index > 0.99), similar to the single aromatic core model compounds and different from the 2 or 3 aromatic core model compounds studied here. These asphaltenes studied here contain ~50% aromatic carbon (comparable to typical asphaltenes[22]), within the range of single aromatic core model compounds but outside the range of 2 or 3 aromatic core model compounds studied here.

Figure 8 plots the stability index versus the H/C ratio. The information contained in this plot is similar to that in Figure 7, which is to be expected given the general relationship between aromaticity and H/C ratio. Asphaltenes (stability index > 0.99)

Table 3. Abundance of the Parent Ion Peak in the Mass Spectrum for Archipelago (A) and Island (I) Compounds

model compound	parent peak abundance (%)
A-1	92
A-2	55
A-3	80
A-4	29
A-5	38
A-6	27
A-7	30
A-8	87
A-9	85
A-10	27
I-1	100
I-2	100
I-3	93
I-4	94
I-5	78
I-6	100
I-7	100
I-8	92
I-9	65
I-10	100
I-11	100
I-12	100
I-13	100

Figure 4. L^{2}MS spectrum of a mixture with a molar ratio equal to 2:1 asphaltenes/I-8. This ratio was determined by approximating the molecular mass of asphaltenes as the mass at which the L^{2}MS molecular-mass distribution peaks, 750 Da. L^{2}MS is 2.5 times more sensitive to asphaltenes then I-8. The molecular-mass distribution of asphaltenes was not affected by the presence of I-8. When these results are taken with Figure 3, they suggest that SPI L^{2}MS is nearly equally sensitive to most components of asphaltenes.
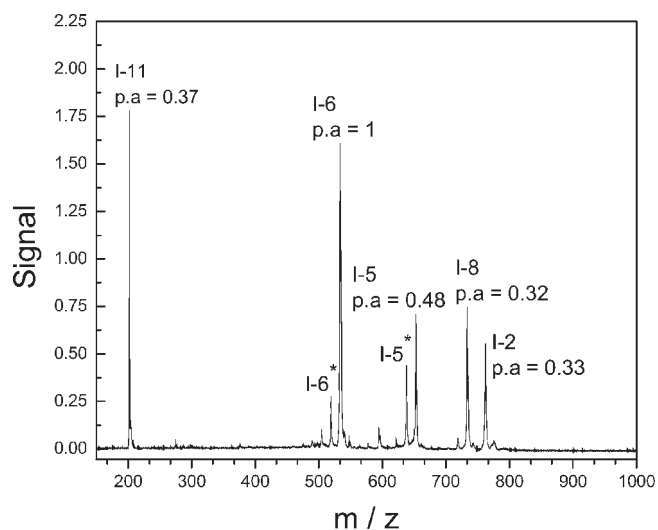

Figure 3. L^{2}MS spectrum of an equimolar mixture of five different model compounds. Asterisks denote fragments of the indicated parent ions. Normalized peak area (pa) for each compound was calculated and indicated on the figure. In cases where fragmentation occurs, the normalized pa is the sum of the normalized pa of the parent ion peak plus its related fragmentation peaks. This figure shows the ability of SPI L^{2}MS to measure the molecular-mass distribution of a synthetic mixture.

Figure 5. L^{2}MS spectra of BG5 asphaltenes recorded at different ionization laser pulse energies using single-photon ionization at 157 nm. Note that the asphaltene average molecular weight is near 600, with an upper limit near 1500.

compounds were studied over the H/C range of 0.7−0.9, and none has stability indices similar to asphaltenes (all <0.9).

have H/C ratios of ∼1.1, comparable to typical asphaltenes. Single aromatic core model compounds were studied over the H/C range of 0.5−1.5, and all have stability indices similar to asphaltenes (all >0.98). The 2 or 3 aromatic core model
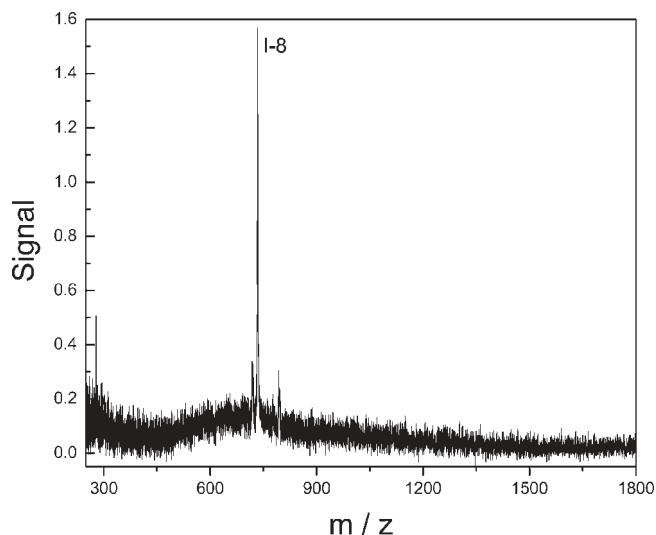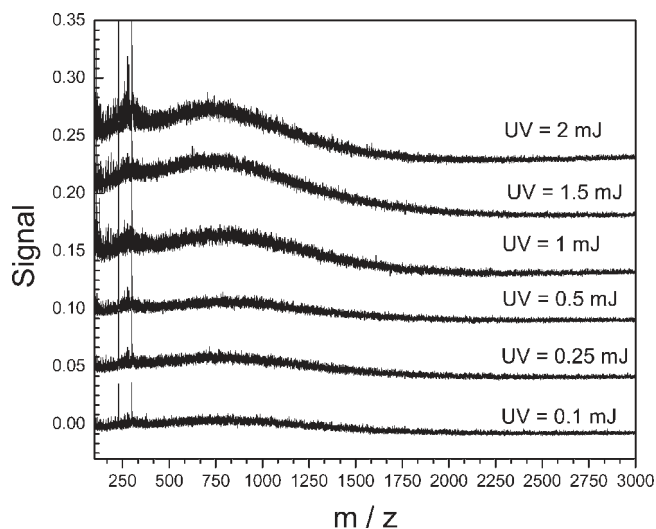
■ DISCUSSION

In this work, we introduced SPI using fluorine excimer laser output at 157 nm as a new ionization source for L^{2}MS and applied it to examine the mass spectra of 2 asphaltene samples and 23 different model compounds. The fluorine excimer laser is able to ionize, by means of single-photon ionization, compounds
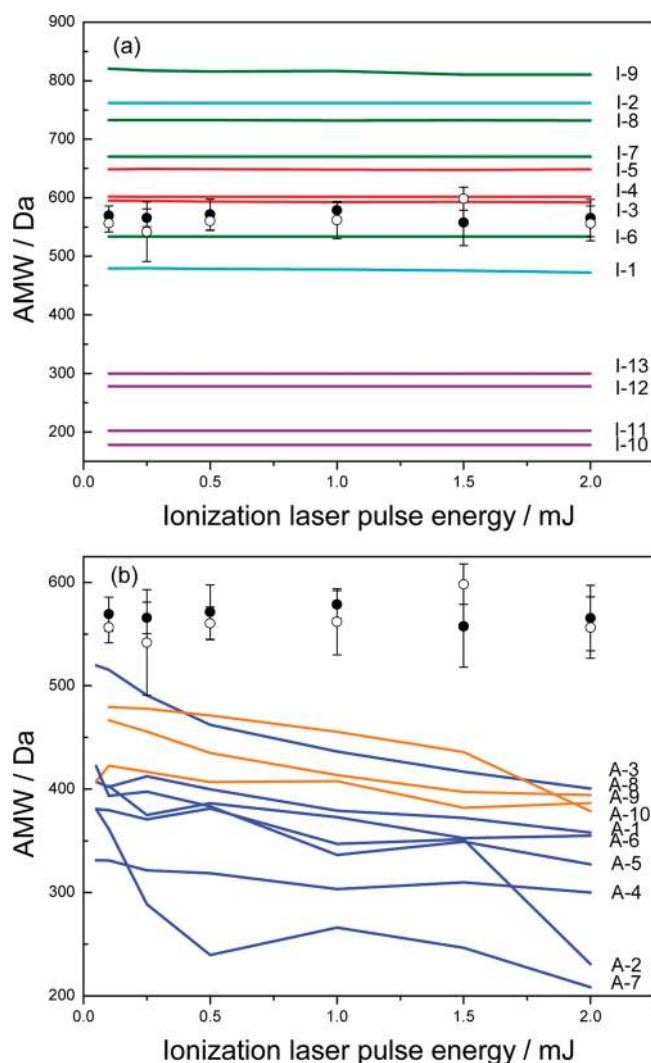
Figure 6. Fragmentation behavior of different compounds as a function of ionization laser pulse energy: (a) island compounds and (b) archipelago compounds. Black dots, BG5 asphaltenes; open dots, UG8 asphaltenes; blue lines, linked-pyrene model compounds; orange lines, linked-phenanthrene model compounds; red lines, cholestanones; cyan lines, single-pyrene model compounds; green lines, porphyrins; and purple lines, PAHs.

having ionization potentials less than 7.89 eV. It represents a softer ionization source than $[1 + 1]$ REMPI with the fourth harmonic output of a Nd:YAG laser at 266 nm, which was used in previous L^{2}MS studies.

We found that the fluorine excimer ionization source is able to detect the parent ion in all compounds studied, that all model compounds studied are detected with approximately the same sensitivity, that asphaltenes are detected with comparable similarity to the model compounds, and that this ionization source provides an accurate estimate of the molecular-mass distribution of simple synthetic mixtures. Thus, we feel confident that the SPI L^{2}MS instrument was able to detect the majority of components found in asphaltenes and to make an accurate measurement of the asphaltene molecular-mass distribution. In particular, the fact that the singly charged parent ion was easily detected for each compound studied suggests that L^{2}MS provides an accurate estimate of the upper limit of the asphaltene molecular-weight distribution.
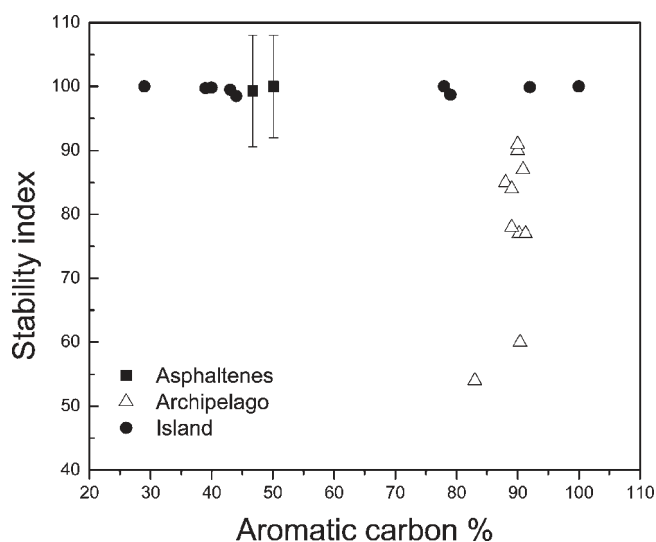

Figure 7. Plot shows the stability index of compounds in SPI L^{2}MS versus their aromatic carbon percentage. The stability index is equal to the AMW at the lowest ionization pulse energy divided by the AMW at the highest ionization laser pulse energy. Compounds with a single aromatic core are found to have high stability, regardless of aromatic carbon percentage, similar to asphaltenes. Compounds with 2 or 3 aromatic cores are found to have lower stability than asphaltenes, but only a small range of aromatic carbon percentages was studied.
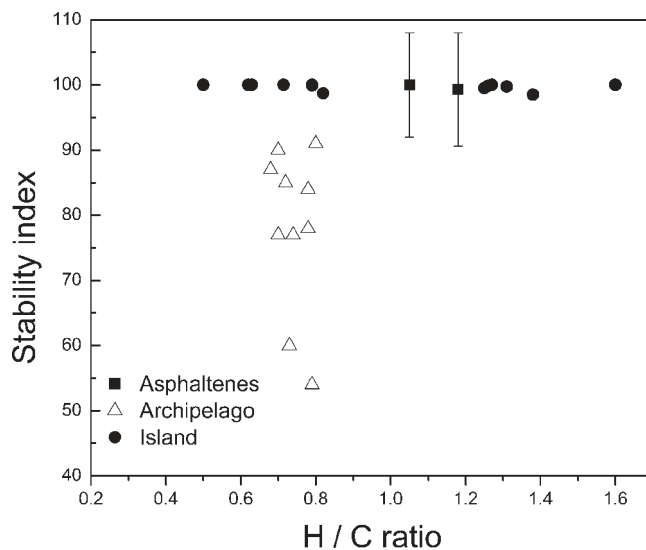

Figure 8. Plot shows the stability index of compounds in SPI L^{2}MS versus their H/C ratio. The stability index is equal to the AMW at the lowest ionization laser pulse energy divided by the AMW at the highest ionization laser pulse energy. Compounds with a single aromatic core are found to have high stability, regardless of H/C ratio, similar to asphaltenes. Compounds with 2 or 3 aromatic cores are found to have lower stabilities than asphaltenes, but only a small range of H/C ratios was studied.

We found that the mass spectra from two asphaltene samples were essentially independent of laser pulse energy over the range from 0.1 to 2.0 mJ/pulse; that is, they display little detectable fragmentation. A similar study of the fragmentation pattern as a function of ionization laser pulse energy was made of six different

families of model compounds. We observe that all studied model compounds that have single aromatic cores are stable in L^{2}MS over the energy range studied and exhibit a similar behavior to asphaltenes. On the other hand, all studied model compounds with 2 or 3 aromatic cores connected by other groups fragment relatively easily over the same range of laser pulse energies.

On the basis of the observations presented in this work, we reach the following two conclusions: (1) 1500 Da is the upper limit to the molecular mass for components of asphaltenes, and the average mass is around 600 Da. (2) The candidate model compounds having 2 or more aromatic cores can be ruled out as representative of asphaltenes.

Several previous studies have addressed the question of what is the dominant molecular architecture of asphaltenes. One of the earliest was that by Groenzin and Mullins,[9,12] who measured the time-dependent depolarization of asphaltene fluorescence. They found that asphaltene molecules that fluoresce in the blue region of the electromagnetic spectrum depolarize about 10 times more rapidly than those that fluoresce in the red. On the basis of simple ideas of a particle in a box, they associate the blue fluorescence to originate from smaller conjugated systems than the red fluorescence. Because the blue and red fluorescence depolarize at different rates, owing to rotational diffusion in solution, it is concluded that the blue and red fluorescent systems are not locked to cause them to rotate at a common rate. Questions remain about whether internal rotation might still allow for these two systems to be associated nevertheless and about how representative these blue and red fluorescing molecules are of all of the asphaltenes present, but these measurements point to the island model as being dominant.

Another germane study was carried out by Borton et al.,[23] who examined the mass spectrometric fragmentation behavior of many of the same model compounds as studied here using electron impact ionization. This ionization method places much more energy into the ions than SPI L^{2}MS. They concluded they were unable to differentiate unambiguously between island- and archipelago-type structures, although their results are in a better agreement with the island model.

A major question is whether the 23 model compounds that we have examined, which cover 6 different structural families, are typical of what might be expected to be present in asphaltenes. To the extent that they are, the present results provide evidence for the dominance of the island model (the Yen−Mullins model). We regard this finding not as proof for the architecture of asphaltenes but as strongly suggestive.

■ AUTHOR INFORMATION

Corresponding Author

*Telephone: +650-723-3062. E-mail: zare@stanford.edu.

■ REFERENCES

(1) Hortal, A. R.; Hurtado, P.; Martinez-Haya, B.; Mullins, O. C. Molecular-weight distributions of coal and petroleum asphaltenes from laser desorption/ionization experiments. *Energy Fuels* **2007**, *21*, 2863–2868.

(2) Hortal, A. R.; Martinez-Haya, B.; Lobato, M. D.; Pedrosa, J. M.; Lago, S. On the determination of molecular weight distributions of asphaltenes and their aggregates in laser desorption ionization experiments. *J. Mass Spectrom.* **2006**, *41*, 960–968.

(3) Klein, G. C.; Kim, S.; Rodgers, R. P.; Marshall, A. G. Mass spectral analysis of asphaltenes. I. Compositional differences between pressure-drop and solvent-drop asphaltenes determined by electrospray ionization Fourier transform ion cyclotron resonance mass spectrometry. *Energy Fuels* **2006**, *20*, 1965–1972.

(4) Klein, G. C.; Kim, S.; Rodgers, R. P.; Marshall, A. G.; Yen, A. Mass spectral analysis of asphaltenes. II. Detailed compositional comparison of asphaltenes deposit to its crude oil counterpart for two geographically different crude oils by ESI FT-ICR MS. *Energy Fuels* **2006**, *20*, 1973–1979.

(5) Martinez-Haya, B.; Hortal, A. R.; Hurtado, P.; Lobato, M. D.; Pedrosa, J. M. Laser desorption/ionization determination of molecular weight distributions of polyaromatic carbonaceous compounds and their aggregates. *J. Mass Spectrom.* **2007**, *42*, 701–713.

(6) Mullins, O. C. The modified Yen model. *Energy Fuels* **2010**, *24*, 2179–2207.

(7) Pomerantz, A. E.; Hammond, M. R.; Morrow, A. L.; Mullins, O. C.; Zare, R. N. Asphaltene molecular-mass distribution determined by two-step laser mass spectrometry. *Energy Fuels* **2009**, *23*, 1162–1168.

(8) Rodgers, R. P.; Schaub, T. M.; Marshall, A. G. Petroleomics: MS returns to its roots. *Anal. Chem.* **2005**, *77*, 20A–27A.

(9) Groenzin, H.; Mullins, O. C. Asphaltene molecular size and structure. *J. Phys. Chem. A* **1999**, *103*, 11237–11245.

(10) Murgich, J.; Abanero, J. A.; Strausz, O. P. Molecular recognition in aggregates formed by asphaltene and resin molecules from the Athabasca oil sand. *Energy Fuels* **1999**, *13*, 278–286.

(11) Sheremata, J. M.; Gray, M. R.; Dettman, H. D.; McCaffrey, W. C. Quantitative molecular representation and sequential optimization of Athabasca asphaltenes. *Energy Fuels* **2004**, *18*, 1377–1384.

(12) Groenzin, H.; Mullins, O. C. Molecular size and structure of asphaltenes from various sources. *Energy Fuels* **2000**, *14*, 677–684.

(13) Sabbah, H.; Morrow, A. L.; Pomerantz, A. E.; Mullins, O. C.; Tan, X. L.; Gray, M. R.; Azyat, K.; Tykwinski, R. R.; Zare, R. N. Comparing laser desorption/laser ionization mass spectra of asphaltenes and model compounds. *Energy Fuels* **2010**, *24*, 3589–3594.

(14) Pomerantz, A. E.; Hammond, M. R.; Morrow, A. L.; Mullins, O. C.; Zare, R. N. Two-step laser mass spectrometry of asphaltenes. *J. Am. Chem. Soc.* **2008**, *130*, 7216–7217.

(15) Hahn, J. H.; Zenobi, R.; Zare, R. N. Subfemtomole quantitation of molecular adsorbates by two-step laser mass spectrometry. *J. Am. Chem. Soc.* **1987**, *109*, 2842–2843.

(16) Kovalenko, L. J.; Philippoz, J. M.; Bucenell, J. R.; Zenobi, R.; Zare, R. N. Organic chemical analysis on a microscopic scale using two-step laser desorption multiphoton ionization mass spectrometry. *Space Sci. Rev.* **1990**, *56*, 191–195.

(17) Deckert, A. A.; George, S. M. Heating rates required for laser-induced thermal-desorption studies of surface-reaction kinetics. *Surf. Sci.* **1987**, *182*, L215–L220.

(18) Sherman, M. G.; Kingsley, J. R.; McIver, R. T., Jr.; Hemminger, J. C. Laser-induced thermal desorption with Fourier transform mass spectrometric detection. *Catalyst Characterization Science*; American Chemical Society (ACS): Washington, D.C., 1985; ACS Symposium Series, Vol. 288, Chapter 21, pp 238−251.

(19) Verstraete, L.; Leger, A.; Dhendecourt, L.; Dutuit, O.; Defourneau, D. Ionization cross-section measurements for 2 PAH molecules—Implications for the heating of diffuse interstellar gas. *Astron. Astrophys.* **1990**, *237*, 436–444.

(20) Hanley, L.; Zimmermann, R. Light and molecular ions: The emergence of vacuum UV single-photon ionization in MS. *Anal. Chem.* **2009**, *81*, 4174–4182.

(21) Wiley, W. C.; McLaren, I. H. Time-of-flight mass spectrometer with improved resolution. *Rev. Sci. Instrum.* **1955**, *26*, 1150–1157.

(22) Buenrostro-Gonzalez, E.; Groenzin, H.; Lira-Galeana, C.; Mullins, O. C. The overriding chemical principles that define asphaltenes. *Energy Fuels* **2001**, *15*, 972–978.

(23) Borton, D.; Pinkston, D. S.; Hurt, M. R.; Tan, X.; Azyat, K.; Scherer, A.; Tykwinski, R.; Gray, M.; Qian, K; Kenttämaa, H. I. Molecular structures of asphaltenes based on the dissociation reactions of their ions in mass spectrometry. *Energy Fuels* **2010**, *24*, 5548–5559.